Iranian Journal of Astronomy and Astrophysics
Vol. 10, No. 3, Summer 2023, 253–265
©Available online at http://ijaa.du.ac.ir
DOI: 10.22128/ijaa.2023.705.1154
Online ISSN: 2383–403X

Iranian Journal of Astronomy and Astrophysics

Research Paper

TR Jets above Magnetic X-Type Null Points

Ehsan Tavabi*[1] · Mehri Heidari[2] · Azam Mollatayefeh[3]

[1] Physics Department, Payame Noor University, Tehran, Iran, 19395–3697;
*email: e_tavabi@pnu.ac.ir

[2] Physics Department, Payame Noor University, Tehran, Iran;
email: mehri.heidari.zanjan@gmail.com

[3] Physics Department, Payame Noor University, Tehran, Iran;
email: azam.mollatayefeh@gmail.com

Received: 16 August 2023; **Accepted:** 6 November 2023; **Published:** 27 November 2023

Abstract. Various chromosphere and transition region jet-like structures abound playing an essential role in the dynamics and evolution therein. Tentatively identifying the wave characteristics and oscillatory behavior in the outer solar atmosphere helps to understand this layer better. For the last decades, the search for the origin of the X-ray and EUV brightening related to the jet-like activity is the subject of hundreds studies because their relevance to the heating problem and the storage of mass inside the corona and the wind sources. In addition to the whip-like behavior, null-point motions in the reconnection site can excite transversal oscillation along the jets, which is called the kink mode wave, and also this mode can evolve into Alfven wave after its propagation into the more homogeneous medium. The study of X-ray jets is an important topic in understanding the heating of the solar corona and the origin of the fast wind. The recently launched Hinode mission permitted to observe the excellent proxies of these jets with an unprecedented high spatial resolution of 120 km on the Sun. We selected a high cadence sequence of SOT (Hinode) observations taken with both the HCaII and the Halpha filter to look at the details of the dynamics revealed by a significant jet event. Both wavelet and amplitude spectra analysis were used to analyze the observed kink wave and the time variations of intensities during the event. The results are discussed in the frame of different models implying reconnections with the inference of the dynamical phenomena occurring near several null points, including the oscillatory behavior.

Keywords: Chromospheric Jets, Magnetic Null Point, Reconnection

1 Introduction

Jets are tiny and straight threads-like structures which are always seen in the transition region (TR). Furthermore chromosphere; those were first seen by Secchi (1877) [1]. The spectra of Mg II k & h, C II, Ca II H, and Si IV clearly show these structures [2–8]. About twenty-three years later, Pike and Mason (1998) discovered that those macro-spicules that produce blue and red shifts in the opposite direction have a spiral motion [9]. A spicule that appears to differ from previous findings in terms of speed, angle, and direction of movement

* *Corresponding author*

was seen throughout this research on spicules. It seems that these spicules are caused by vorticity movements, which can also be the reason of the propagation of Alfven rotational waves and the transfer of energy to the Sun's upper atmosphere. To continue, it should be noted that the observational resolution of the different observations in this study varies and that rotating spicules are tiny structures visible in extremely high-resolution observations. A wide range of dynamic phenomena occurs in the solar atmosphere, including the upper parts where the magnetic field dominates. However, the soft X-Ray ejections and specific energetic macro-flares have been associated with the magnetic reconnection process that appears in a 3D topology at a magnetic null point, consisting of a fan located below the null point and a spine field line above it (e.g., Priest & Forbes 2000) [10]. Under the potential or near-potential magnetic topology, a 3-D null-point general configuration with a fan plane and a spine axis is seen if a magnetic bi-pole structure is embedded into one polarity region of a large-scale bi-polar ambient field [11]. It is commonly approved that reconnections are appropriate for explaining features such as particle acceleration and plasma heating. The exotic properties of X-type neutral points have played a central role in developing X-Ray coronal dynamics. Current sheets accumulate magnetic energy at null points in the plasma, and provide sites for strong magnetic energy release [10]. Craig & Fabling (1996) suggested that current sheets are associated mainly with three-dimensional fan-current reconnection [12]; other reconnection models require quasi-cylindrical spine currents that develop along the exhaust axis of the fluid [13]. Almost all jets have been classified into two groups:
(i) Cool chromospheric jet-like structures such as spikes, surges, and small-scale anemone jets ([14–17]),
(ii) Hot magnetic plasma ejection, such as W-L, EUV and X-ray coronal jets ([16,18–20]).
Alfven and magnetoacoustic wave modes may exist, though these are normally coupled together. Nullpoint motions in an axially symmetric system can excite transversal oscillation, which is called the kink mode wave. Also, this mode can evolve into an Alfven wave after its propagation into the more homogeneous medium [21]. Upward propagating waves are generally exploited in theoretical models for heating the chromosphere and the corona [22]. Rickard & Titov (1996) Have studied the cold plasma, using linear, resistive, magnetohydrodynamic (MHD) an equation to study the dynamics of current accumulation at a three-dimensional magnetic null [23]. Their theoretical analysis shows that the axis-symmetric perturbations for $m = 0$ (where m is the azimuthal wave number) can lead to a current parallel to the spine axis at the null and corresponds to topological reconnection, while the $m = 1$ mode produces currents orthogonal to the spine axis at the null (parallel to the fan plane), and for $m > 1$, there is never any current at the null [24]. Dynamically, we know that $m = 0$ corresponds to toroidal oscillations propagating along the zero-order field lines and eventually localized parallel to the spine axis with a cylindrical column of current aligned to this axis. The $m = 1$ mode produces motions across both the fan and spine axis in single null point events, resulting in a current distribution wholly in the fane plane. One of the most important efficient $m = 1$ mode concentrates magnetic flux toward the null and produces strong currents in the fan plane. It is possible that in the system of this theoretical study, which remains cold plasma, the evolution of neutral points and currents is never seen explicitly in a hot coronal hole X-ray jets or the whip-like motion, which is interpreted as a slingshot-like motion and is the result of reconnections which make some elaborated motions detected as transversal motion of coronal hole X-ray jets.

2 Observations

2.1 Data reduction and Image processing

The Hinode SOT (SOT is poised to address many critical questions about MHD) data taken above the solar limb have been utilized to figure out the dynamical nature of the incredible jets. HCaII images in this research were taken from the Broad-band Filtergram Imager (BFI) of SOT/Hinode and the Halpha series from the Narrowband Filter Imager (NFI) [25]. The observational resolution of Hinode/Halpha is half that of Hinode/H Ca II, which explains we don't notice rotation in the spicules. The size of all frames that were utilized

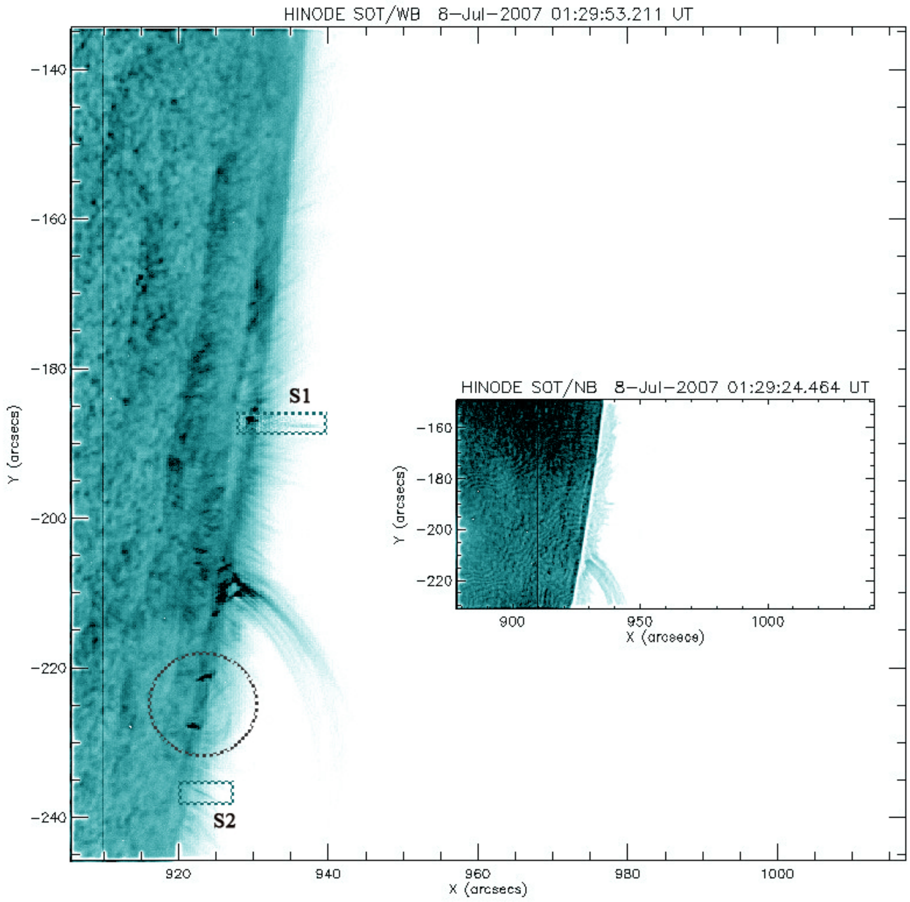

Figure 1: Selective image in the negative intensity of HCaII and Halpha images showing a typical cool macro-jet; obtained Halpha filtergram is seen inserted in the Ca band; times are in U.T. (the left vertical thin line is due to the CCD two parts), dotted circle demonstrate a double base of mini chromosphere loop.

here is 1024×512 pixels^2 (SOT/Hinode readout only the central line of the detector to keep the best cadence within the teleportation) thus covering an area of (FOV) 111x56. The SOT/Hinode observations were calibrated with 'fg_ prep' of the solar software [26]. An unprecedented high spatial image processing for straight-line features or aligned features is implemented using the MadMax model [27]. The MadMax convolution tries to enhance the finest features substantially. The MadMax filter is a weakly non-linear convolution of a second-derivative spatial operator. Primarily, it is applying the second derivative has a maximum than looking along all-around directions. The algorithm, as initially proposed, samples the second derivative in eight directions, but the directional variation of the second derivative was generalized. Spatial filtering using MadMax saw relatively bright straight threads all-round the Sun as fine as the diffraction limit of the order of 120 km.

2.2 Feature in detail

The brightening of several loop systems at the edge of a sunspot was observed by SOT for about two-three hours on July 2007, 08 between about 00:34 and 03:11 UT. The dynamic evolution described in the following lasted about one hour, ending at 02:05 UT. Figure 2 & 3 show snapshots outlining the central feature of the jet in both HCaII and Halpha lines simultaneously, at about 01:14 U.T., then the main spine of the jet becomes obvious. The red dashed lines denote that median axes of the that (includes the interchange space), and the double short blue lines show two different heights with a distance of 3 M.m., which henceforth are denoted as layer I & II, and indicate the location on the jet where its transversal displacement is further analyzed.

At about 01:25 UT, the jet becomes more dynamic, and it seems that two or three null points appear close to each other. They appear to have different brightness and collectively exhibit a fine tiny typical jet-like shape as defined by Shibata[17], or an Eiffel tower shape as defined by others. The observation suggests that the dynamic phenomena were caused by the interaction of newly emerging flux in the arcade-like field near the active region. The long-lived phenomenon concentrates in the vicinity of the sunspot, which would have multiple 3D null points during the event. The jet-like phenomena arose as a flash-like feature that propagated along the spine and demonstrated a whip-like motion is seen in the Figure 4; it should be interpreted as a "magnetic reconnection" between small emerging bipole. This slingshot behavior with brightness also includes an amplitude of the transversal oscillatory motion that is perhaps related using a magneto-acoustic wave similar to a propagating kink or an Alfven wave. The propagation of transversal motion across the spine axis is a response of neutrals ions to the collimated magnetic plasma with a specific perturbation along the multiple null point separators (the propagation near the null points and the propagation of transversal wave along the spine is better visible in the online movie accompanying Figures 2 & 3).

3 Data analysis

Figure 4 presents a typical diagram corresponds to temporal sequences of displacements corresponding to the jet's axis. In this figure, we find that points on the jet spine axis oscillate transversally with time; in addition, the average transverse motion around the central longitudinal spine axis shows a whip-like motion from left to right in both layers. The fourier analysis illustrated two dominant peaks around 2, 3, and 5 mHz; 3. 3 mHz frequency could be related to photospheric high-frequency oscillation and 5 mHz should interpret as chromosphere 180 sec. Typical oscillation.

Wavelet high-frequency fast Fourier transform (FFT) analysis are now used to obtain temporal spectra. In Figure 5, the two top plots show the wavelet time-frequency analysis power spectra for intensity time fluctuations for layers I & II, which were shown in time-slice diagrams of transversal wave oscillations; the bottom plot shows the (gray plot).

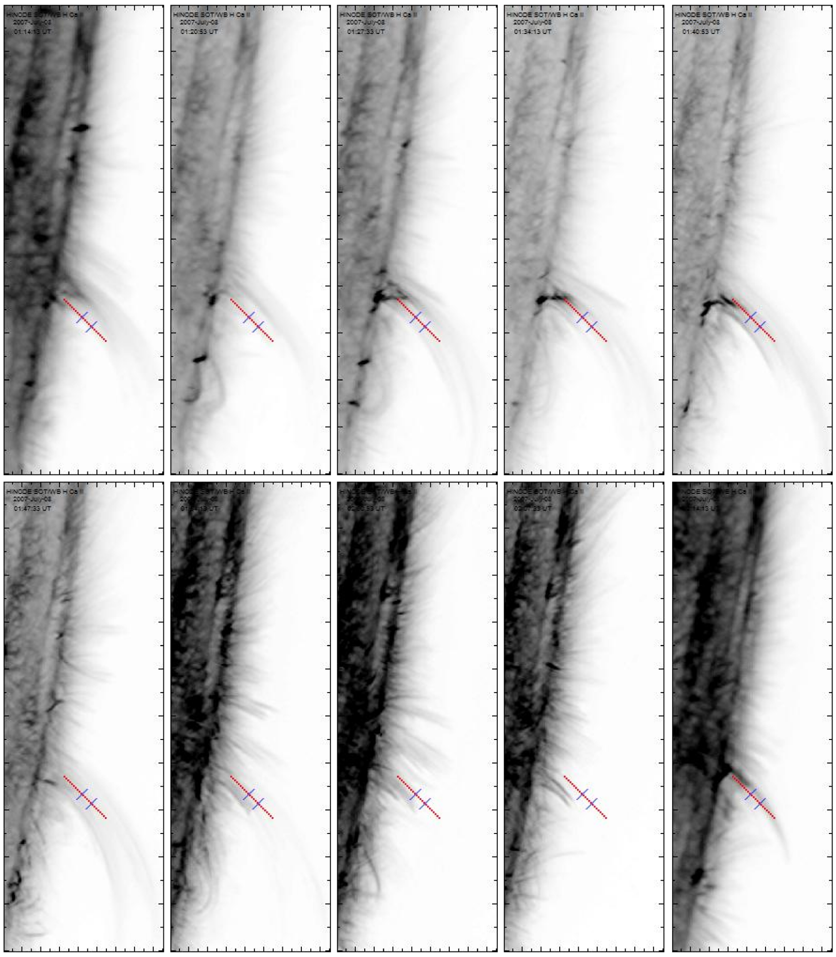

Figure 2: Negative and Madmaxed frames from the SOT/Hinode Broad-band HCaII filter observations (25×65 arcsec^2) at different times (01:14 to 2:14 UT). The spine axis (includes interchange space) is denoted by a red line. Blue lines are plotted at layer-I & II positions in all images to outline the oscillatory transverse motion and displacement of its central part. See the text for details. (An avi animation of this figure is available in the online journal). The animation uses a different intensity scaling, which outlines the jet more clearly.

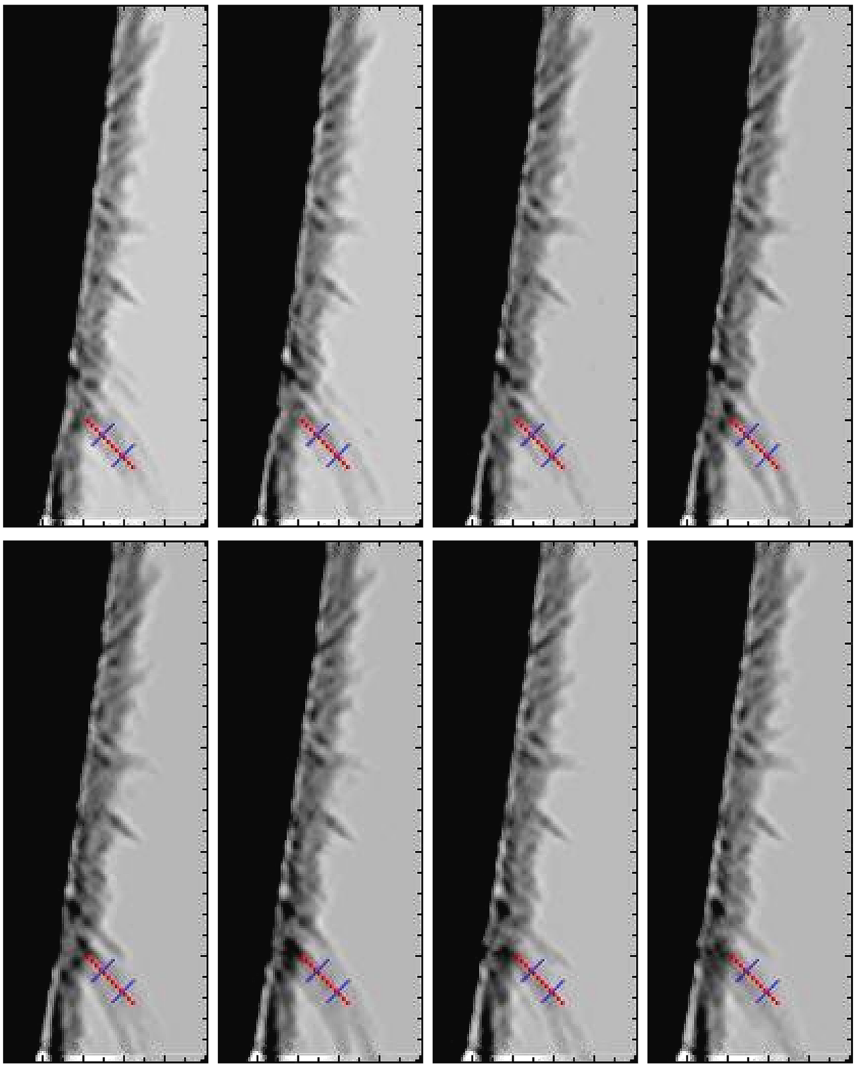

Figure 3: Selected snapshots of negative and mad-maxed images from the SOT narrowband Halpha filter observations (35×105 arcsec^2) at different times (01:14 to 2:14 UT). The spine axis (includes interchange space) is denoted by the dashed red line. Blue lines are plotted at layer-I & II positions in all images to outline the oscillatory transverse motion and displacement of its central part. See the text for details (an avid animation of this figure is available in the online journal). The animation uses a different intensity scaling, which outlines the jet more clearly.

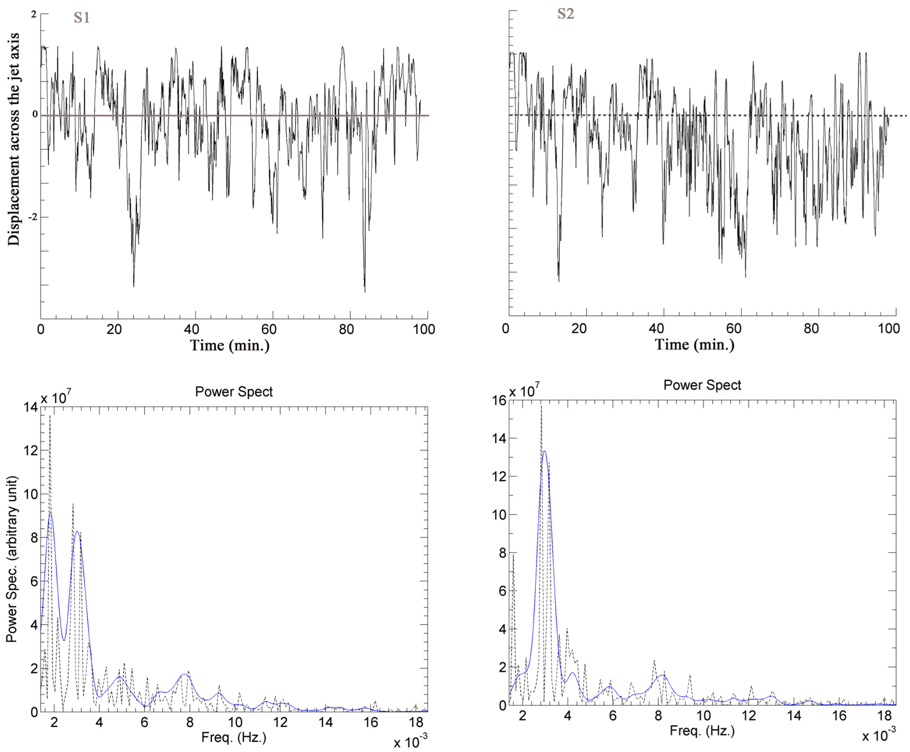

Figure 4: A sample of intensity oscillation of incredible jets (top) and their oscillatory frequencies using the Fast Fourier Transform (bottom) correspondence to S1 and S2 regions that marked in Figure 1.

Furthermore, the phase difference (color plot) for the layers corresponding to each other. The horizontal axis is the time in minutes, while the vertical axis is the period in minutes. Darker shades correspond to a higher power (%95 confidence) of the wavelet coefficients. The contours determine the %95 confidence level, which was calculated by assuming a white noise background spectrum. Wavelet transform suffers from the "wraparound" errors at both edges of a time series (of finite length). The region in which these effects are important is defined by the cone of influence (COI; see Torrence and Compo, 1998) [28]. The Cone Of Influence (COI) region, or in other words, demonstrates the region that suffers from edge effects, is chosen as the e-folding time of the Morlet wavelets is presented as a cross-hatched in each plot. From the wavelet time/frequency analysis of intensity fluctuation in these layers, we obtain a typical period of about 3 min which can be related by the chromospheric 3-min oscillations and from the coherency and phase difference diagram, we could find a large coherency in the 2-4 min range, but for more considerable periods, the coherency coefficients decrease. In the observed layers, I & II the phase-difference obtained from the wavelet analysis is reassuring in that it is indeed showing a near-zero degree difference in large part of the time between 2-4 min of period and for another time range part, it reaches a maximum value of about 120 degrees (boundary of blue and red) at 3 min, corresponding to a time delay of 60 Second for these two different layers with a distance between them is about 3 minutes.

FFT analysis is also used to calculate the amplitude spectrum (AS), and it is shown in the middle panels of Figure 6. It is found that the AS has a maximum at five mHz, which corresponds to a period of 180 s, and it confirms the wavelet time/frequency result for both layers. We carry out a cross-correlation analysis of the two oscillation sequences for layers-I & II, in order to evaluate the propagation direction of the oscillation as well as to determine the phase speed. The upper panels of Figure 6 display the transversal oscillation sequences for the two layers, respectively. This oscillation has a maximum cross-amplitude spectrum (CAS) at 2 MHz. The correlation coefficient between oscillations of different layers as a function of the time lag can be obtained by applying an inverse-FFT method to the CAS profile.

The correlation coefficient has a maximum value for the time lag of 1 min, and it is showing that the oscillation for layer II has a time lag of 1 min relative to the layer-I and indicates a wave propagation upward with a phase speed of 30 to 40 kms^{-1} along the spine axis. It should be remarked that the phase speed may be much larger than this amount since we could not distinguish a time lag shorter than 40 s, the cadence of the image being of about 20 s, so this maximum corresponds to the Nyquist frequency.

4 Summary and Discussion

We studied SOT/Hinode data that show high-resolution H Ca II and Halpha filtergrams taken at the solar limb, in the TR and chromosphere, as a first test to understand how cool fast ejections are driven through double or multiple null points and how transversal motions are generated. Suematsu et al. (2008) studied the observation of untwisted motion of spicules from Hinode/SOT achievements, and He et al. (2009) reported a high-frequency transverse motion in spicules, which also agrees with the results of Tavabi et al. (2011) [29–31]. Additional statistically significant parameters should be determined to respond to the key question concerning the origin and driving forces related to the curvature shape looking similar to a transverse kink-mode oscillation along the threads. A kind of collective and quasi-coherent behavior along the spicules was considered for the first time by Tavabi et al. (2011) and Tavabi (2014) [31,32]. Most spicules were found to show impressive trans-

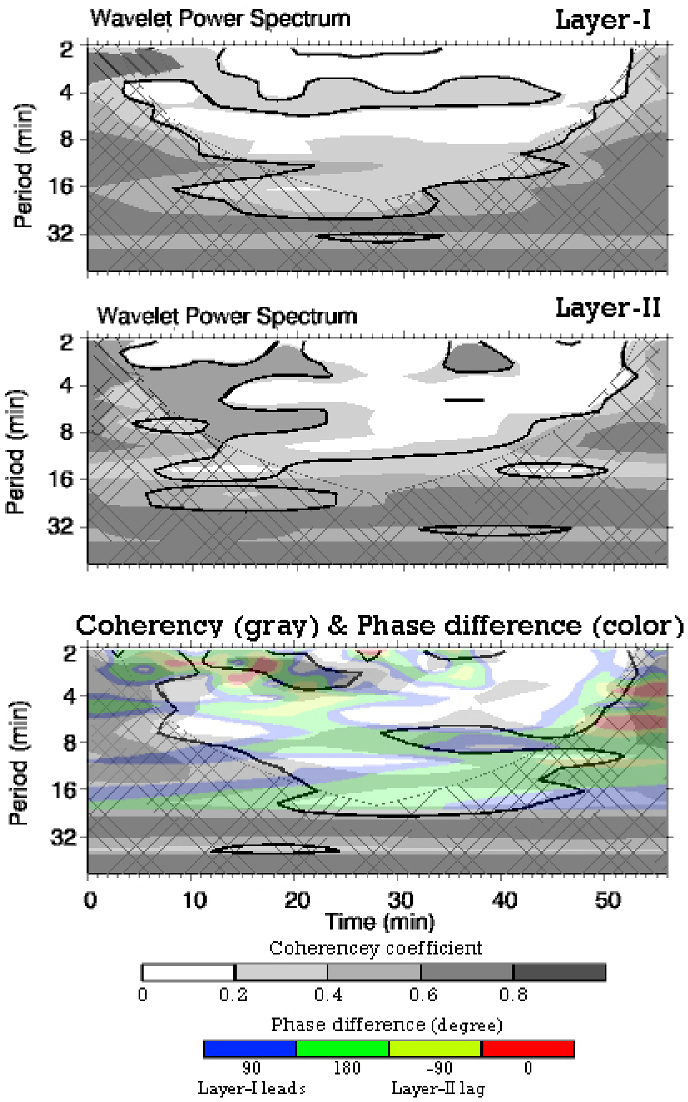

Figure 5: Upper plots show wavelet powers corresponding to the intensity fluctuations (period vs. time) for layer-I & II. The lower plot shows the coherency (gray) and the phase difference (color) plot simultaneously and correspondingly, the color bars for the coherency coefficient (gray) and the phase difference at the bottom. Cross-hatched regions indicate the "cone of influence" (COI). The darkest regions mean a higher power, and the contours correspond to the %95 confidence level (see text and reference for details).

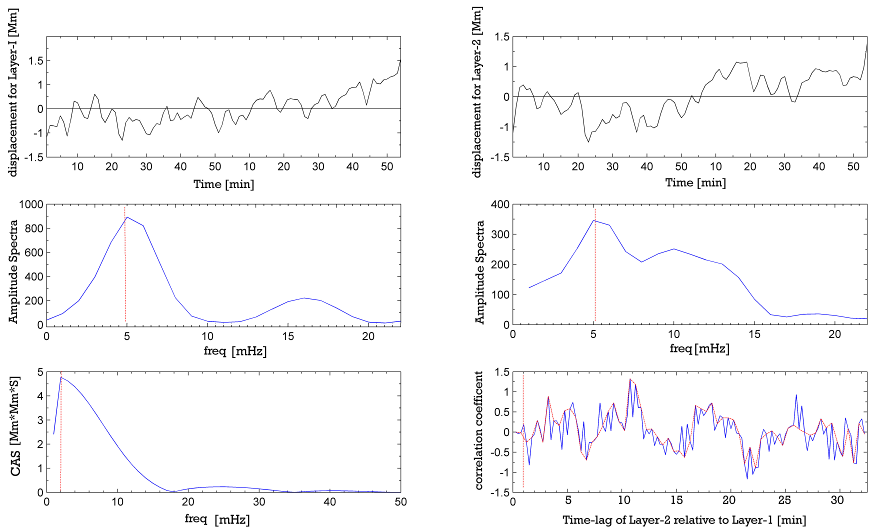

Figure 6: Upper panels: intensity fluctuations for layer- I & II (black lines). Middel panels show amplitude spectra (AS) for these two layers (blue lines), and red vertical lines indicate the maximum oscillation values. In the lower-left panel: cross amplitude spectrum (CAS) for the oscillations of layer-I & II; in the lower right panel: correlation coefficient as a function of the time lag between the oscillation of Layers-I & II, (solid blue line) and the fitting using the 5^{th} Fourier harmonic (red dashed line).

verse periodic behavior, which was interpreted as an upwardly propagating kink mode of transversal magneto-acoustic waves or Alfvén waves. Magnetic cylindrical tubes support transverse waves as kink mode oscillations that perhaps anchored in photospheric magnetic bright points at the boundary of photosphere granules through the buffeting action of granular motions, although the true proxy of the magnetic bright point in the network region toward the corona is still a matter of discussion [33,34].

Shibata et al. (2007) analyzed a small-scale jet in an active region using SOT data [17]. Their events are typically of 3 to 7 arcsec equal to 2 to 5 Mm length, and of 0.35 Mm width and their apparent velocity is 10 to 20 km/s; these small-scale jets have a Lambda shape, similar to the shape of X-ray anemone jets in the corona which have been discovered on the coronal hole by the Yohkoh satellite as transitory X-ray enhancement in the solar corona with collimated motion [16]. Figure 1 shows that the H Ca II large-scale jet is typically of more than 20 arcsec length and has a five arcsec width; these values are much larger than the physical parameter of H Ca II jets reported by Shibata et al. [17]. However, the propagating velocity of our H Ca II jet is similar and about 15 km/s; it is in the range of values was predicted for incredible jets in the low chromosphere and photosphere [35]. We have also provided evidence for jet transversal oscillations across the jet spine. Under azimuthally symmetric ($m = 0$), they are the only modes associated with topological magnetic reconnection, and it is shown that reconnection has to appear in the cases of purely radial perturbations and allows a typical charge current parallel to the spine axis at the null-point [24]. Rickard & Titov (1996) found that the m equal one ($m = 1$) is the most likely transversal mode to naturally reveal the axisymmetric single null point [23]. There are two paths to make this mode, tilting and, as a result in current-sheet accumulation in the separator wall for a time interval that could be related to the transient time, but for the double null-point, it is could just perturb each null with purely $m = 1$, mode by perturbing the spine separator axes. To our knowledge, the propagation of MHD waves in such incredible jets has never been seen; it is similar to what was seen in a coronal hole X-ray jet; for such hot events, only we see the sling-shot motions of the spine axis during their evolution. Our amplitude spectrum analysis also shows apparent, transversal wave propagation inside the jet with a phase speed of up to 50 km/s, comparable to the speed of Alfven wave in the low chromosphere plasma. Our results confirm the theoretical predictions quite well and indicate that the jets have an influential role in heating the higher layers.

Acknowledgments

We thank B. Filippov for useful discussions, and we are very grateful to the Hinode team for providing wonderful observations. Hinode is a Japanese mission developed and launched by ISAS/JAXA, with NAOJ as domestic partner and NASA and STFC (UK) as international partners. Image processing MAD-MAX program was provided by O. Koutchmy; see `http://www.ann.Jussieu.fr/~koutchmy/index\_newE.HTML` and wavelet analysis software was provided by Torrence and Compo (`http://atoc.colorado.edu/research/wavelets`).

Authors' Contributions

All authors have the same contribution.

Data Availability

No data available.

Conflicts of Interest

The authors declare that there is no conflict of interest.

Ethical Considerations

The authors have diligently addressed ethical concerns, such as informed consent, plagiarism, data fabrication, misconduct, falsification, double publication, redundancy, submission, and other related matters.

Funding

This research did not receive any grant from funding agencies in the public, commercial, or nonprofit sectors.

References

[1] Secchi, P. A. 1877, Le Soleil, Vol. 2, Chap. II. Paris: Gauthier-Villars.

[2] De Pontieu, B., McIntosh, S. W., Carlsson, M., Hansteen, V. H., Tarbell, T. D., & et al. 2007, Science, 318, 5856, 1574.

[3] Sterling, A. C., Moore, R. L., & DeForest, C. E. 2010, ApJ, 714, L1.

[4] Madjarska, M. S., Vanninathan, K., & Doyle, J. G. 2011, A&A, 532, L1.

[5] Pereira, T. M. D., De Pontieu, B., Carlsson, M., Hansteen, V., Tarbell, T. D., & et al. 2014, ApJ, 792, L15.

[6] Pereira, T. M. D., De Pontieu, B., & Carlsson, M. 2012, ApJ, 759, 18.

[7] Pereira, T. M. D., Rouppe van der Voort, L., & Carlsson, M. 2016, ApJ, 824, 65.

[8] Beck, T., Tao, Ch., Chen, L., & Frank, S. 2016, Journal of Banking & Finance, 72, 28.

[9] Pike, C. D., & Mason, H. E. 1998, Sol. Phys., 182, 333.

[10] Priest, E. R., & Forbes, T. G. 2000, Magnetic Reconnection, Cambridge Univ. Press, Cambridge.

[11] Antiochos, S. K., 1998, ApJ., 502, L181.

[12] Craig, I. J. D., & Fabling, R. B. 1996, ApJ, 462, 969.

[13] Galsgaard, K., & Nordlund, Å. 1997, J. Geophys. Res., 102(A1), 231.

[14] Sterling, H. C. 2000, Sol. Phys., 196, 79.

[15] Koutchmy, S. & Stellmacher, G. 1976, Sol. phys., 49, 253.

[16] Shibata, K., Ishido, Y., Acton, L., Strong, K., Hirayama, T., & et al. 1992, PASJ, 44, L173.

[17] Shibata, K., Nakamura, T., Matsumoto, T., Otsuji, K., Okamoto, T., & et al. 2007, Science, 318, 1591.

[18] Tsuneta, S. 1997, ApJ, 483, 507.

[19] Filippov, B., Golub, L., & Koutchmy, S. 2009, Sol. Phys., 254, 259.

[20] Koutchmy, S. 1969, Astrophysical Letters, 4, 215.

[21] Cranmer, S. R., van Ballegooijen, A. A., & Edgar, R. J. 2007, ApJS, 171, 520.

[22] Hollweg, J. V., & Isenberg, P. A. 2002, J. Geophys. Res., 107, 1147.

[23] Rickard, G. J., & Titov, V. S. 1996, ApJ, 472, 840.

[24] Craig, I. J. D., & Watson, P. G., 1992, ApJ, 393, 385.

[25] Tsuneta, S., Ichimoto, K., Katsukawa, Y., Nagata, S., Otsubo, M., & et al. 2008, Sol. Phys. ,249, 167.

[26] Shimizu, T., Nagata, S., Tsuneta, S., Tarbell, T., Edwards, C., & et al. 2008, Sol. Phys., in press.

[27] Koutchmy, O., & Koutchmy, S. 1989, in Proc. 10th Sacramento Peak Summer Workshop, High Spatial Resolution Solar Observations, ed. O. von der Luhe (Sunspot: NSO), 217.

[28] Torrence, C., & Compo, G. P. 1998, Bulletin of the American Meteorological Society, 79, 61.

[29] Suematsu, Y., Ichimoto, K., Katsukawa, Y., Shimizu, T., & Okamoto, T. 2008, ASP Conf., 397, 27.

[30] He, J. S., Tu, C. Y., Marsch, E., & et al. 2009, A&A, 497, 525.

[31] Tavabi, E., Koutchmy, S., & Ajabshirizadeh, A. 2011, New Astron., 16, 296.

[32] Tavabi, E. 2014, Astrophys. Space Sci., 352, 43.

[33] Roberts, B. 1979, Solar Phys., 61, 23.

[34] Hasan, S. S., & Kalkofen, W. 1999, ApJ, 519, 899.

[35] Shibata, K. 1997, Proc. 5th SOHO Workshop, Oslo, Norway, [European Space Agency (ESA) SP-404, 1997], 103.